Capture of a diffusing lamb by a diffusing lion when both return home

R. K. Singh [1,*] and Sadhana Singh[2,†]

[1]*Department of Physics, Bar-Ilan University, Ramat-Gan 5290002, Israel*
[2]*The Avram and Stella Goldstein-Goren Department of Biotechnology Engineering,*
Ben-Gurion University of the Negev, Be'er Sheva 84105, Israel

A diffusing lion pursues a diffusing lamb when both of them are allowed to get back to their homes intermittently. Identifying the system with a pair of vicious random walkers, we study their dynamics under Poissonian and sharp resetting. In the absence of any resets, the location of intersection of the two walkers follows a Cauchy distribution. In the presence of resetting, the distribution of the location of annihilation is composed of two parts: one in which the trajectories cross without being reset (center) and the other where trajectories are reset at least once before they cross each other (tails). We find that the tail part decays exponentially for both the resetting protocols. The central part of the distribution, on the other hand, depends on the nature of the restart protocol, with Cauchy for Poisson resetting and Gaussian for sharp resetting. We find good agreement of the analytical results with numerical calculations.

I. INTRODUCTION

Search is a fundamental endeavor to survival ranging from human search [1] to rescue operations [2] to animal foraging [3,4] to protein binding on DNA [5], transcription factors searching for a specific DNA [6,7], to mention a few. A useful search strategy involves intermittent phases of slow motion aiding the searcher in target detection and fast motion allowing the searcher to cover maximal ground in minimal time [8]. Restarting a search process at intermittent intervals, aka stochastic resetting, has been extensively shown to expedite search [9]. Stochastic resetting has been a very active topic of research within the realm of nonequilibrium statistical physics over the past decade [9]. The basic essence of stochastic resetting is that in any kind of search process, the search is rarely successful in the first attempt. Following which the search is restarted again and again until the process culminates with success. This property is common to a wide variety of search processes. Now it is almost always true that if a sufficient amount of time is devoted, then any search shall meet success. The question of value is, however, whether an intermittent restart of the search process tends to reduce the time of completion. The answer to this question is affirmative. At least in the case of stochastic algorithms it has been shown that a simple restart might expedite completion [10–12]. Not only in endeavors of human interest, nature also employs restarts in many processes, for example enzymatic reactions following the Michaelis-Menten reaction scheme [13].

The idea of stochastic resetting to the Brownian search problem was first applied in the seminal work of Evans and Majumdar [14]. They showed that restarting a Brownian particle to its initial location at a constant rate renders the mean first passage time (MFPT) finite. The process of restarting a stochastic process at a constant rate is termed as Poissonian resetting. In addition to Brownian motion, Poissonian resetting has been applied to run and tumble particles [15], fluctuating interfaces [16], dynamical phase transitions [17,18], resetting transitions [19,20], telegraphic processes [21], comblike structures [22,23], multiple Brownian searchers [24], etc. However, Poissonian resetting is not exclusive and other protocols such as power-law distributed resetting times [25], resetting rates depending on space [26] and time [27] have also been extensively studied. This raises an interesting question: given the wide class of resetting protocols, does there exist a reset mechanism under which MFPT is minimal? This question is difficult to answer in its full generality. However, when resetting is renewal, then sharp resetting in which the time interval between two resets is fixed serves as the best strategy [28,29]. In other words, "if there exists a stochastic resetting protocol that improves search process, then there exists a deterministic restart protocol that performs as good or better" [30].

Poissonian and sharp restarts lie at the two extremes of renewal resetting, the former being memoryless and the latter retaining its entire memory. Both these protocols were compared against each other for a system of Brownian particles searching for a target in Ref. [31] and it was shown that sharp resetting typically leads to a lower search cost than that in Poissonian resetting. This study was taken further for a system of Brownian particles where interactions are relevant, for example, in population genetics [32]. The inclusion of interactions further allows one to consider more nontrivial forms of resetting mechanisms such as those which are driven by the interactions between the constituent particles [33] or space-dependent resetting in interacting Brownian particles [34]. One of the most important examples which involves

---

interacting random walks is the well-known prey predator model which culminates when the prey is captured by the predator [35]. An exactly solvable prey predator model with resetting was recently considered by Evans and coworkers [36] where the prey on its encounter with a predator can either perish or be reset to its initial location.

In the present work we consider the prey predator model within the realm of vicious random walks which annihilate each other the moment their trajectories cross [37]. The concept was first introduced by Fisher in the context of interfacial wetting in $1 + 1$ dimensions [38,39] and has since been applied to Coulomb gas [40] and random matrices [41]. The survival probability for vicious random walkers in one dimension exhibits power-law decaying tails [42], and any two such walkers shall certainly meet each other as a random walk in one dimension is recurrent [43,44]. The problem of reunion of two vicious random walks corresponds to the chemical reaction $A + A \rightarrow \phi$ [45] and is one of the most classic problems in nonequilibrium statistical physics [46–48]. The annihilating nature of the vicious walkers makes them suitable for studying directed polymer brushes wherein the viciousness captures the role of the nonintersecting property of polymers [49]. Vicious random walks have also been applied to breathing DNA with the collapse of the bubbles viewed as an annihilation of two vicious walkers moving in opposite potentials [50]. Furthermore, the distribution of the location of coalescence makes it relevant to study the location where the trajectories of two vicious walkers cross. In the context of the capture problem where a hungry lion pursues a lamb [51], the location of intersection tells us how far the hunt is made from the home. The scenario also makes the concept of resetting very natural [52]. This is because either the lamb shall every now and then return to its home, or the lion to its den, or both. The reason that such a thing might happen is the lion pursues the lamb but could not catch it and gets tired eventually getting back in its cave. On the other hand, the freely roaming lamb might spot the lion and run away from it. This makes the study of vicious random walks under resetting very natural. In other words, if we have two vicious Brownian particles we want to know how long do they survive without crossing each other's paths? And if their trajectories cross, what is the nature of the distribution of such a point? Do the answers to these questions depend on the resetting protocol employed? We address these questions in the following sections by studying the system of two vicious Brownian particles under resetting. The particles are reset identically to their respective initial positions either at constant rates (Poissonian resetting) or after fixed time intervals (sharp resetting).

II. TWO VICIOUS RANDOM WALKERS

Consider two Brownian particles:

$$\dot{x}_1 = \eta_1(t), \tag{1a}$$

$$\dot{x}_2 = \eta_2(t), \tag{1b}$$

where $\eta_1(t), \eta_2(t)$ are independent Gaussian random deviates with mean zero and delta correlated variance, that is, $\langle \eta_1(t)\eta_1(t') \rangle = 2D_1\delta(t - t')$ and $\langle \eta_2(t)\eta_2(t') \rangle = 2D_2\delta(t - t')$. At $t = 0$ the two walkers are at $x_1 = 0$ and $x_2 = L$. The

two walkers annihilate each other as soon as their paths cross, that is, $x_1(t) = x_2(t)$. The problem is readily transformed to the motion of the center of mass $x_c = \frac{x_1+x_2}{2}$ and relative separation of the two particles $x_r = x_1 - x_2$. In terms of the new coordinates, the center of mass moves as a free Brownian particle as

$$\dot{x}_c(t) = \eta_c(t), \tag{2}$$

where $\langle \eta_c(t) \rangle = 0$ and $\langle \eta_c(t)\eta_c(t') \rangle = 2D_c\delta(t - t')$ with $D_c = \frac{D_1+D_2}{4}$. On the other hand, the relative coordinate x_r moves like a Brownian particle on line

$$\dot{x}_r(t) = \eta_r(t), \tag{3}$$

where $\langle \eta_r(t) \rangle = 0$ and $\langle \eta_r(t)\eta_r(t') \rangle = 2D_r\delta(t - t')$ with $D_r = D_1 + D_2$. Before the trajectories of the two particles cross, the center of mass exhibits a Brownian motion centered at $x_c = L/2$ with a diffusion coefficient D_c and the relative coordinate is a Brownian particle starting at $x_r = -L$ with an absorbing wall at $x_r = 0$. The first passage time distribution (FPTD) of the relative coordinate to the absorbing wall at $x_r = 0$ is $F(t) = \frac{L}{\sqrt{4\pi D_r t^3}} \exp\left(-\frac{L^2}{4D_r t}\right)$ and the probability density function (PDF) of the center-of-mass motion is $p(x_c, t) = \frac{1}{\sqrt{4\pi D_c t}} \exp\left[-\frac{(x_c-L/2)^2}{4D_c t}\right]$ [53,54]. From the FPTD it is evident that the mean time to the annihilation of the two vicious walkers $\langle t \rangle = \int_0^\infty dt\, t\, F(t)$ is infinite. The recurrence of a Brownian motion in one dimension, however, implies that the two walkers will eventually collide, and the PDF of the location of intersection is

$$h(x_c) = \int_0^\infty dt\, F(t)p(x_c, t)$$

$$= \frac{1}{\pi} \frac{L/\sqrt{D_r D_c}}{\frac{L^2}{D_r} + \frac{(x_c-L/2)^2}{D_c}}, \tag{4}$$

which is a Cauchy distribution centered at $x_c = L/2$. Similar to the MFPT, there is no well-defined mean location of the intersection of the two vicious walkers. This is because even though the two walkers shall certainly meet, they may take a really long time to do so by venturing out in opposite directions resulting in the divergence of MFPT and a well-defined mean location of annihilation. In other words, the hungry lion may keep pursuing the lamb forever and might eventually die of hunger. And this is where resetting comes in to prevent the hungry lion from dying.

III. RESETTING TO INITIAL CONFIGURATION

With the vector (x_1, x_2) defining the system, define a resetting protocol: after an interval of reset time τ the system is reverted back to its initial configuration. The time τ is either an exponentially distributed random variable (Poissonian resetting) or a fixed quantity (sharp resetting). For simplicity let us assume that the two walkers are reset via identical resetting protocols at the exact same time. The reason for this choice is the following: let us assume that the two walkers are reset at different times τ_1 and τ_2; then a scenario is possible in which $\tau_1 < \tau_2$ and $x_1(\tau_1) < x_2(\tau_2) < 0$ just before reset has taken place. The moment after the reset we have $x_1(\tau_1) > x_2(\tau_2)$ which apparently means that the two trajectories have crossed

paths. Such crossing of two walkers is, however, erroneous as at the time of reset the first particle is removed from its current location and put back to its initial location instantaneously. This makes the intersection point an ill-defined quantity simply for the reason that actual trajectories did not cross. We avoid such a pathological situation by requiring that the two particles be reset at the exact same time. Furthermore, restarting the two walkers identically retains the advantage that the two-particle system is still described by the motion of the center of mass and motion about the center of mass. Next we consider the two resetting protocols one by one.

A. Poissonian resetting

Let the two walkers be reset to their respective initial locations at a rate R. Then the FPTD of the relative coordinate under Poissonian resetting is [52]

$$\tilde{F}_R(s) = \frac{\tilde{F}(s+R)}{\frac{s}{s+R} + \frac{R}{s+R}\tilde{F}(s+R)}, \tag{5}$$

where $\tilde{F}(s) = \int_0^\infty dt\, e^{-st} F(t) = \exp(-\sqrt{sL^2/D_r})$ is the Laplace transform of the FPTD without resetting [55]. From this follows the MFPT under Poissonian resetting as $\langle \mathscr{T}_R \rangle = \frac{e^{\sqrt{RL^2/D_r}} - 1}{R}$. This result has been previously derived in [14] via the backward Fokker-Planck equation and many works following it. Here we state the result as a reminder that MFPT under Poissonian resetting is finite.

In order to study the effect of resetting on the PDF of the intersection of the two trajectories, we need the FPTD $F_R(t)$ given in terms of the Bromwich integral [56]:

$$\begin{aligned}
F_R(t) &= \frac{1}{2\pi i} \int_{\gamma-i\infty}^{\gamma+i\infty} ds\, \frac{(s+R)e^{-\alpha L}}{s + Re^{-\alpha L}} e^{st}, \\
&\stackrel{\text{large } t}{\approx} \frac{1}{2\pi i} \int_{\gamma-i\infty}^{\gamma+i\infty} ds\, \frac{Re^{-z}}{s + Re^{-\alpha L}} e^{st},
\end{aligned} \tag{6}$$

where $\alpha = \sqrt{\frac{s+R}{D_r}}$ and $z = \sqrt{R/D_r}L$. While the exact inversion of $\tilde{F}_R(s)$ is possible [57], for our purposes the long time behavior of $F_R(t)$ suffices. This integral is easily evaluated from the residue of $\tilde{F}_R(s)$ at the pole closest to $s = 0$. The pole of $\tilde{F}_R(s)$ is given by the solution of $s + Re^{-\alpha L} = 0$ which in terms of $s = R(u-1)$ reads [14]

$$u = 1 - e^{-\sqrt{u}z}, \tag{7}$$

and has a unique nonzero solution $u_0 \in (0, 1)$. Thus, the FPTD at large times is [14]

$$\begin{aligned}
F_R(t) &\stackrel{\text{large } t}{\approx} \lim_{s \to s_{0,R}} e^{st}(s - s_0)\tilde{F}_R(s) \\
&= \frac{2R\sqrt{u_0}e^{-z}}{2\sqrt{u_0} - z(1-u_0)} e^{s_{0,R}t},
\end{aligned} \tag{8}$$

where $s_{0,R} = R(u_0 - 1) < 0$ implying that at large times the FPTD under resetting possesses exponentially decaying tails. This result is verified numerically and a good agreement is found for the characteristic decay exponent $s_{0,R}$ as shown in Fig. 1(a). Next, we estimate the PDF of the center-of-mass
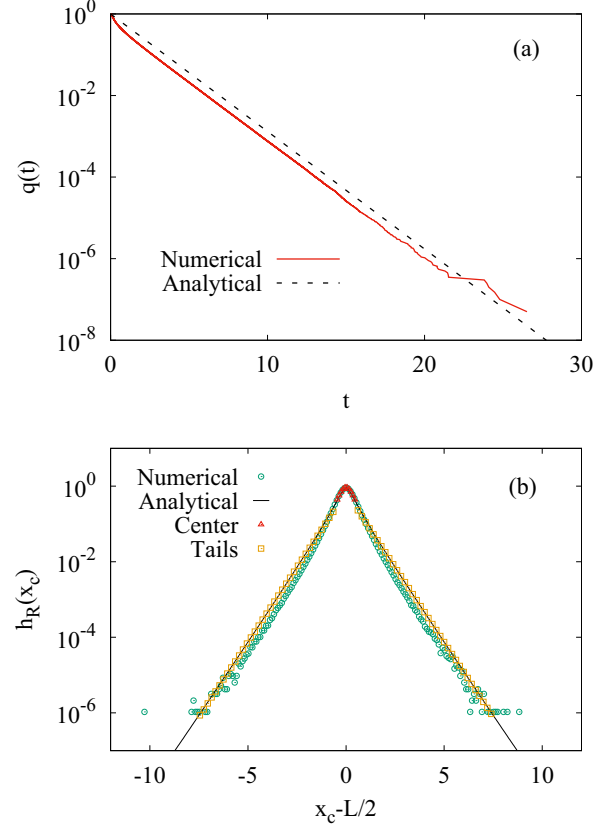

FIG. 1. (a) Survival probability $q(t)$ for the two vicious walkers following Eq. (1) to not cross paths up to time t reset to their initial positions at a constant rate R. Red solid line represents numerically estimated $q(t)$ while the black dashed line represents the analytical form $q(t) \sim \exp(-|s_{0,R}|t)$. (b) Numerically estimated PDF of the location of intersection $h_R(x_c)$ (green circles) is compared against the approximate form in Eq. (13) (black solid line). Yellow squares denote the contribution to h_R^t for $|x_c - L/2| > L/2$ and red triangles h_R^c for $|x_c - L/2| < L/2$. We have used a factor b such that $h_R \sim bh_R^c$ to demonstrate that h_R^c indeed captures the center of h_R (up to a scale). Parameter values are $D_1, D_2 = 1$, $L = 1$, $R = 1$, and $b = 2$.

motion under resetting, following the renewal equation [9]

$$p_R(x_c, t) = e^{-Rt}p(x_c, t) + \int_0^t d\tau\, Re^{-R\tau}p(x_c, \tau), \tag{9}$$

where the first term gives the contribution from the trajectories which have not been reset at all, while the second term describes the effect of resetting. As a result, the PDF of the intersection point of the two vicious walkers under Poissonian resetting annihilating each other with FPTD $F_R(t)$ is

$$\begin{aligned}
h_R(x_c) &= \int_0^\infty dt\, F_R(t)p(x_c, t)e^{-Rt} \\
&\quad + \int_0^\infty dt\, F_R(t)\int_0^t d\tau\, Re^{-R\tau}p(x_c, \tau) \\
&\equiv h_R^c(x_c) + h_R^t(x_c),
\end{aligned} \tag{10}$$

where h_R^c denotes the single integral and h_R^t denotes the double integral. In what follows we shall see that h_R^c having the contribution of intersection points without reset captures the

central part of the PDF h_R. While h_R^t describes the tails consisting of the intersection points with reset, hence the usage of the superscripts c and t, respectively. Let us now proceed to evaluate the two integrals in (10) one by one.

For the single integral in Eq. (10), $F_R(t) = F(t) = \frac{L}{\sqrt{4\pi D_r t^3}} \exp\left(-\frac{L^2}{4D_r t}\right)$, since the system behaves like the one without resetting. Furthermore, if we look at the FPTD under Poissonian resetting, that is, $\tilde{F}_R(s) = \frac{(s+R)e^{-\alpha L}}{s+Re^{-\alpha L}}$, then at small times $\tilde{F}_R(s) \overset{\text{large } s}{\approx} \exp\left[-L\sqrt{\frac{s+R}{D_r}}\right] \Rightarrow F_R(t) \overset{\text{small } t}{\approx}$ $F(t)e^{-Rt}$, which is exactly the same quantity as appearing in the first integral in (10). In other words, the probability of crossing of two trajectories without being reset is e^{-Rt}, effectively modifying the FPTD entering in the evaluation of $h_R^c(x_c)$. Hence, we have

$$h_R^c(x_c) = \frac{1}{\pi}\sqrt{\frac{RL^2}{L^2 D_c + (x_c - L/2)^2 D_r}}$$
$$\times K_1\left[\sqrt{R\left\{\frac{L^2}{D_r} + \frac{(x_c - L/2)^2}{D_c}\right\}}\right], \tag{11}$$

where K_1 is the modified Bessel function of the second kind and it enters while evaluating the Laplace transform of $e^{-1/t}$ [55]. The double integral in (10) is similarly evaluated:

$$h_R^t(x_c) \approx \int_0^\infty dt\, A(s_{0,R}) e^{s_{0,R}t} \int_0^t d\tau\, Re^{-R\tau} p(x_c, t)$$
$$= \frac{RA(s_{0,R})}{\sqrt{4\pi D_c}} \int_0^\infty d\tau \frac{1}{\sqrt{\tau}} e^{-R\tau - a/\tau} \int_\tau^\infty dt\, e^{-|s_{0,R}|t}$$
$$= \frac{RA(s_{0,R})/|s_{0,R}|}{\sqrt{4D_c(|s_{0,R}| + R)}} \exp\left(-\sqrt{\frac{|s_{0,R}| + R}{D_c}}\left|x_c - \frac{L}{2}\right|\right), \tag{12}$$

where $a = \frac{(x_c - L/2)^2}{4D_c}$ and $A(s_{0,R}) = \frac{2R\sqrt{u_0}e^{-z}}{2\sqrt{u_0} - z(1-u_0)}$. Combining the results in (11) and (12) we have

$$h_R(x_c) \approx \frac{1}{\pi}\sqrt{\frac{RL^2}{L^2 D_c + (x_c - L/2)^2 D_r}}$$
$$\times K_1\left[\sqrt{R\left\{\frac{L^2}{D_r} + \frac{(x_c - L/2)^2}{D_c}\right\}}\right]$$
$$+ \frac{RA(s_{0,R})/|s_{0,R}|}{\sqrt{4D_c(|s_{0,R}| + R)}} \exp\left[-\sqrt{\frac{|s_{0,R}| + R}{D_c}}\left|x_c - \frac{L}{2}\right|\right]. \tag{13}$$

From Eq. (13), it is evident that h_R^c describes the center and h_R^t the tails of the PDF h_R. This is due to the rapid decay of the modified Bessel function as compared to exponential. Furthermore, for small arguments K_1 decays algebraically, that is, $K_1(w) \overset{\text{small } w}{\sim} 1/w$ [58], from where it follows that $h_R^c(x_c)$ behaves like a Cauchy distribution. Thus, when the two walkers are reset to their initial locations at a constant rate, the PDF h_R exhibits a Cauchy distributed center and exponentially

decaying tails. In other words, Poissonian resetting of the two walkers reduces the fat tails of the PDF to the center and the far tails are modified to exponential. In summary,

$$h_R(x_c) \approx \begin{cases} \frac{1}{\pi} \frac{L/\sqrt{D_r D_c}}{\frac{L^2}{D_r} + \frac{(x_c - L/2)^2}{D_c}}, & \text{center,} \\ \frac{RA(s_{0,R})/|s_{0,R}|}{\sqrt{4D_c(|s_{0,R}| + R)}} \exp\left[-\sqrt{\frac{|s_{0,R}| + R}{D_c}}\left|x_c - \frac{L}{2}\right|\right], & \text{tails.} \end{cases} \tag{14}$$

We compare the analytically estimated PDF h_R in Eq. (13) (black solid line) with numerical calculations (green circles) in Fig. 1(b) and find that they are in close proximity.

The contribution to the PDF coming from h_R^c in the range $|x_c - L/2| < L/2$ is scaled by a factor b to match the numerically estimated h_R. The reason for doing this is to show that h_R^c indeed captures the shape of the center of the PDF. The tail part h_R^t in region $|x_c - L/2| > L/2$ matches well with numerically estimated h_R as following the similar decay rate as shown in Fig. 1(b). Here, we refer to the region $|x_c - L/2| < L/2$ as the central part. The simple reason for the usage of this terminology is that the center of mass is midway between the two vicious particles and an annihilation taking place within this region would simply mean that the center of mass has not ventured far from its mean position.

B. Sharp resetting

In sharp resetting, the two walkers are reset to their respective initial locations after fixed intervals of time T. In order to estimate the FPTD under sharp resetting, we use the results derived by Pal and Reuveni in Ref. [28]. They show that if τ is the time of completion of a stochastic process without restart, and ρ is the time interval of restart, then the FPTD under restart reads [28]

$$\tilde{F}_{\text{res}}(s) = \frac{\Pr(\tau < \rho)\tilde{\tau}_{\min}(s)}{1 - \Pr(\rho \leqslant \tau)\tilde{\rho}_{\min}(s)}, \tag{15}$$

where $\rho_{\min} = \{\rho | \rho = \min(\rho, \tau)\}$ is the random restart time given restart occurred before completion and $\tau_{\min} = \{\tau | \tau = \min(\rho, \tau)\}$ is the random completion time without any restarts. For Poissonian resetting when ρ is an exponentially distributed random variable, that is, $f_\rho(t) = Re^{-Rt}$, Eq. (15) reduces to (5) (see Supplemental Material in Ref. [28]). For sharp resetting at fixed intervals of time T, the distribution of restart times ρ is $f_\rho(t) = \delta(t - T)$. As a result,

$$\Pr(\tau < \rho)\tilde{\tau}_{\min}(s) = \langle e^{-s\tau}\rangle$$
$$= \int_0^\infty dt\, f_\tau(t) \int_t^\infty dt'\, f_\rho(t') e^{-st}$$
$$= \left(\int_0^T + \int_T^\infty\right) dt\, f_\tau(t) e^{-st} \int_t^\infty dt'\, \delta(t' - T)$$
$$= \int_0^T dt\, f_\tau(t) e^{-st}. \tag{16}$$

The $\int_T^\infty$ integral in the third line does not contribute anything as the limits of integration do not contain the point $t' = T$. In a similar manner

$$\Pr(\rho \leqslant \tau)\tilde{\rho}_{\min}(s) = e^{-sT} \int_\tau^\infty dt\, f_T(t). \tag{17}$$

Using (16) and (17) in Eq. (15) we find that the FPTD of a stochastic process under sharp restart is given by

$$\tilde{F}_T(s) = \frac{\int_0^T dt\, f_\tau(t) e^{-st}}{1 - e^{-sT} \int_T^\infty dt\, f_\tau(t)}, \tag{18}$$

where $f_\tau(t)$ is the FPTD without restart and the subscript T on the left-hand side denotes the time of sharp restart T. From the FPTD in (18) follows the MFPT under sharp restart:

$$\langle \mathscr{T}_T \rangle = -\frac{d}{ds}\tilde{F}_T(s)\Big|_{s=0} = \frac{\int_0^T dt\, q_\tau(t)}{\int_0^T dt\, f_\tau(t)}, \tag{19}$$

which has been earlier derived in Ref. [27,30] in an alternative manner with $q_\tau(t)$ denoting the survival probability.

For the system of two vicious random walkers $f_\tau(t) = F(t) = \frac{L}{\sqrt{4\pi D_r t^3}} \exp\left(-\frac{L^2}{4D_r t}\right) \Rightarrow q_\tau(t) = \mathrm{erf}\left(\frac{L}{\sqrt{4D_r t}}\right)$ [54]. Using these in (19) we have the MFPT to annihilation under sharp resetting

$$\langle \mathscr{T}_T \rangle = \frac{\sqrt{\frac{L^2 T}{\pi D_r}} e^{-L^2/4D_r T} - \frac{L^2}{2D_r}\mathrm{erfc}\left(\frac{L}{\sqrt{4D_r T}}\right) + T\,\mathrm{erf}\left(\frac{L^2}{\sqrt{4D_r T}}\right)}{\mathrm{erfc}\left(\frac{L}{\sqrt{4D_r T}}\right)}. \tag{20}$$

The integral of $q_\tau(t)$ above has been evaluated using the integral representation of the error function and related Laplace transforms [55,59]. Once again it is evident that resetting gives a finite MFPT. Next we look at the PDF of the intersection point.

In order to evaluate the PDF of the intersection point under sharp resetting, we need the time domain representation of FPTD in Eq. (18). Using $F(t) = \frac{L}{\sqrt{4\pi D_r t^3}} \exp\left(-\frac{L^2}{4D_r t}\right)$ we have

$$\begin{aligned} F_T(t) &= \frac{1}{2\pi i} \int_{\gamma-i\infty}^{\gamma+i\infty} ds \left[\frac{\int_0^T dt\, F(t) e^{-st}}{1 - e^{-sT} \int_T^\infty dt\, F(t)}\right] e^{st} \\ &\overset{\mathrm{large}\ t}{\approx} \frac{1}{2\pi i} \int_{\gamma-i\infty}^{\gamma+i\infty} ds \left[\frac{\int_0^T dt\, F(t)}{1 - e^{-sT} \int_T^\infty dt\, F(t)}\right] e^{st} \\ &= \frac{1}{2\pi i} \int_{\gamma-i\infty}^{\gamma+i\infty} ds\, \frac{\mathrm{erfc}\left(\frac{L}{\sqrt{4D_r T}}\right)}{1 - e^{-sT}\mathrm{erf}\left(\frac{L}{\sqrt{4D_r T}}\right)} e^{st}, \quad (21) \end{aligned}$$

where we have used the approximation $\int_0^T dt\, F(t) e^{-st} \approx \int_0^T dt\, F(t)$ in the limit of large times t (small s behavior). The integral is now straightforwardly evaluated from the pole in the complex plane located at $s_{0,T} = \frac{1}{T}\ln\mathrm{erf}\left(\frac{L}{\sqrt{4D_r T}}\right)$. As a result

$$F_T(t) \overset{\mathrm{large}\ t}{\approx} \frac{1}{T}\frac{\mathrm{erfc}\left(\frac{L}{\sqrt{4D_r T}}\right)}{\mathrm{erf}\left(\frac{L}{\sqrt{4D_r T}}\right)} e^{s_{0,T}(t+T)} \tag{22}$$

which implies that at large times $F_T(t)$ decays exponentially as $s_{0,T} < 0$, since $\mathrm{erf}\left(\frac{L}{\sqrt{4D_r T}}\right) < 1\ \forall T > 0$. We numerically estimate the characteristic decay time in Fig. 2(a) and find good agreement with the analytical result. Now we estimate the PDF of the center of mass under sharp resetting. When the two vicious walkers are reset to their initial locations regularly after interval T, the number of renewals taking place up to time equals $\lfloor \frac{t}{T} \rfloor$ ($\lfloor \rfloor$ denotes the floor function). Furthermore,
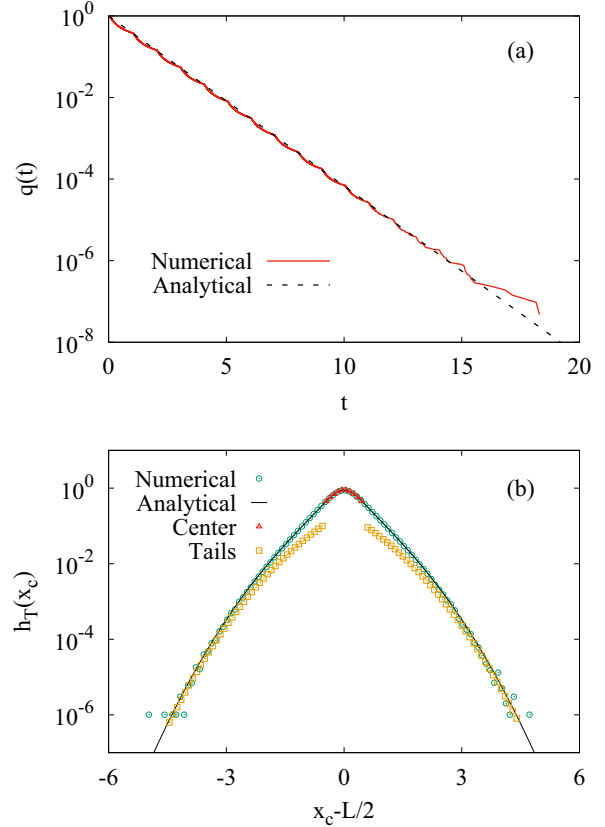

FIG. 2. (a) Survival probability $q(t)$ for the two vicious walkers following Eq. (1) to not cross paths upto time t sharply reset to their initial positions after time T. Red solid line represents numerically estimated $q(t)$ while the black dashed line represents the analytical form: $q(t) \sim \exp(-|s_{0,T}|t)$. (b) Numerically estimated PDF of the location of intersection $h_T(x_c)$ (green circles) is compared against the approximate form in Eq. (24) (black solid line). Yellow squares denote the contribution to h_T^t for $|x_c - L/2| > L/2$ and red triangles h_T^c for $|x_c - L/2| < L/2$. We have used a factor b such that $h_T \sim b h_T^c$ to demonstrate that h_T^c indeed captures the center of h_T (upto a scale). Parameter values are: $D_1,\ D_2 = 1,\ L = 1,\ T = 1$ and $b = 0.4$

since the center of mass starts afresh after every reset, its PDF at time t is given by

$$p_T(x_c, t) = \frac{1}{\sqrt{4\pi D_c\left(t - \lfloor \frac{t}{T} \rfloor T\right)}} \exp\left[-\frac{(x_c - L/2)^2}{4D_c\left(t - \lfloor \frac{t}{T} \rfloor T\right)}\right]. \tag{23}$$

For $t < T$ we have $\lfloor \frac{t}{T} \rfloor = 0$ and the center of mass evolves with the PDF $p(x_c, t)$. If the trajectories of the two walkers cross before any restart, then the time of their annihilation follows the FPTD $F(t)$. As a result, similar to the case of Poissonian resetting, the PDF of the intersection point is composed of two parts: one coming from the trajectories which annihilate each other at $t < T$, and the remaining ones which undergo at least one reset event before crossing their paths. Thus, the PDF of the intersection point under sharp resetting

is

$$h_T(x_c) = \int_0^T dt\, F(t) p(x_c, t) + \int_T^\infty dt\, F_T(t) p_T(x_c, t)$$
$$\equiv h_T^c(x_c) + h_T^t(x_c), \qquad (24)$$

where h_T^c and h_T^t denote the integrals in the intervals $[0, T]$ and $[T, \infty)$, respectively, and are defined analogous to their Poissonian counterparts. The first integral is relatively straightforward and evaluates to

$$h_T^c(x_c) = \frac{1}{\pi} \frac{L/\sqrt{D_r D_c}}{\frac{L^2}{4D_r} + \frac{(x_c - L/2)^2}{4D_c}} \exp\left[-\frac{1}{T}\left\{\frac{L^2}{4D_r} + \frac{(x_c - L/2)^2}{4D_c}\right\}\right]. \qquad (25)$$

This implies that under sharp resetting the fat tails of the Cauchy distribution are tamed to an effective Gaussian. It becomes even more interesting once we realize that here we are considering those trajectories which have not even reset once. In other words, the fact that a restart is set to take place

at $t = T$, forces a certain fraction of trajectories to cross their paths, thus introducing Gaussian cutoffs in the tails. In addition, the central part of the PDF close to the initial location of the center of mass is Gaussian. Now coming to the second integral in (24), we have

$$h_T^t(x_c) \approx \frac{1}{\sqrt{4\pi D_c T^2}} \frac{\mathrm{erfc}\left(\frac{L}{\sqrt{4D_r T}}\right)}{\mathrm{erf}\left(\frac{L}{\sqrt{4D_r T}}\right)} e^{-|s_{0,T}|T}$$
$$\times \int_T^\infty dt\, \frac{\exp\left[-\frac{(x_c - L/2)^2}{4D_c\left(t - \lfloor \frac{t}{T}\rfloor T\right)} - |s_{0,T}|t\right]}{\sqrt{t - \lfloor \frac{t}{T}\rfloor T}}, \quad (26)$$

where the limits of integration are kept from T to ∞ for reasons stated above. The integral in (26) can be evaluated by decomposing the interval of integration into subintervals of length T. This helps us to reduce the integral on the real line $[T, \infty)$ to an integration over the interval $[0, T]$. The reason we can do this is that the floor function turns $t - \lfloor \frac{t}{T}\rfloor T$ into a periodic function. As a result

$$\int_T^\infty dt\, \frac{\exp\left[-\frac{(x_c-L/2)^2}{4D_c\left(t - \lfloor \frac{t}{T}\rfloor T\right)} - |s_{0,T}|t\right]}{\sqrt{t - \lfloor \frac{t}{T}\rfloor T}} = \sum_{m=1}^\infty e^{-|s_{0,T}|mT} \int_0^T dw\, \frac{1}{\sqrt{w}} e^{-(a/w)-|s_{0,T}|w}$$
$$= \frac{\sqrt{\pi/|s_{0,T}|}}{e^{|s_{0,T}|T} - 1}\left[e^{-2\sqrt{a|s_{0,T}|}} - \frac{e^{-2\sqrt{a|s_{0,T}|}}}{2}\mathrm{erfc}\left(\frac{T\sqrt{|s_{0,T}|} - \sqrt{a}}{\sqrt{T}}\right)\right.$$
$$\left. - \frac{e^{2\sqrt{a|s_{0,T}|}}}{2}\mathrm{erfc}\left(\frac{T\sqrt{|s_{0,T}|} + \sqrt{a}}{\sqrt{T}}\right)\right], \qquad (27)$$

where $a = \frac{(x_c - L/2)^2}{4D_c}$ and the integral is evaluated using MAXIMA. This implies that the PDF of the intersection point has exponentially decaying tails for large a. Using (27) in (26) and then along with (25) in Eq. (24) we have

$$h_T(x_c) \approx \begin{cases} \frac{1}{\pi} \frac{L/\sqrt{D_r D_c}}{\frac{L^2}{4D_r} + \frac{(x_c - L/2)^2}{4D_c}} \exp\left[-\frac{1}{T}\left\{\frac{L^2}{4D_r} + \frac{(x_c - L/2)^2}{4D_c}\right\}\right], & \text{center}, \\ \frac{\sqrt{\pi/|s_{0,T}|}}{\sqrt{4\pi D_c T^2}} \frac{\mathrm{erfc}\left(\frac{L}{\sqrt{4D_r T}}\right)}{\mathrm{erf}\left(\frac{L}{\sqrt{4D_r T}}\right)} \frac{e^{-|s_{0,T}|T}}{e^{|s_{0,T}|T}-1}\left[e^{-2\sqrt{a|s_{0,T}|}} - \frac{e^{-2\sqrt{a|s_{0,T}|}}}{2}\mathrm{erfc}\left(\frac{T\sqrt{|s_{0,T}|}-\sqrt{a}}{\sqrt{T}}\right) - \frac{e^{2\sqrt{a|s_{0,T}|}}}{2}\mathrm{erfc}\left(\frac{T\sqrt{|s_{0,T}|}+\sqrt{a}}{\sqrt{T}}\right)\right], & \text{tails}. \end{cases} \qquad (28)$$

We numerically study the PDF of the intersection point in Fig. 2(b) and find that Eq. (24) agrees well with numerical calculations. Furthermore, the PDFs h_T^c (with a scale factor b) and h_T^t also individually agree with the numerically estimated h_T in their respective ranges (as stated above in the case of Poissonian resetting). While it may not be apparent from Fig. 2(b), the tails of h_T are indeed exponential. This follows from the fact that in Eq. (27) the second erfc term describing the tails approaches a constant for large fluctuations, while the third term approaches zero. As a consequence, $h_T^t \sim e^{-2\sqrt{a|s_{0,T}|}}$ for large $|x_c - L/2|$.

IV. COMPARING POISSON RESETTING AND SHARP RESETTING

So far we have studied the dynamics of two vicious walkers under Poissonian and sharp resetting, but in separate

scenarios. It thus becomes interesting to compare the two protocols against each other. The answer to this question is known partly in that sharp resetting wins over Poissonian resetting in the renewal resetting scenario [28]. Hence we compare the minima of the MFPTs under the two resetting protocols. For this purpose let us choose $D_1, D_2 = 1$ and $L = 1$. As a result we have

$$\langle \mathscr{T}_R \rangle = \frac{\exp(\sqrt{R/2}) - 1}{R}, \qquad (29a)$$

$$\langle \mathscr{T}_T \rangle = \sqrt{\frac{T}{2\pi}} \frac{\exp(-1/8T)}{\mathrm{erfc}(1/\sqrt{8T})} + T\frac{\mathrm{erf}(1/\sqrt{8T})}{\mathrm{erfc}(1/\sqrt{8T})} - \frac{1}{4}. \qquad (29b)$$

From the above equations, the minima of the MFPT $\langle \mathscr{T}_R \rangle$ occurs at $R = R_0$ where $\frac{d}{dR}\langle \mathscr{T}_R\rangle|_{R=R_0} = e^{\sqrt{R_0/2}}/\sqrt{8R_0^3} - \langle \mathscr{T}_{R_0}\rangle/R_0 = 0 \Rightarrow R_0 \approx 5.079$. For this value of the resetting rate $\langle \mathscr{T}_{R_0} \rangle \approx 0.772$. Similarly, $\langle \mathscr{T}_T \rangle$ has a global minima at
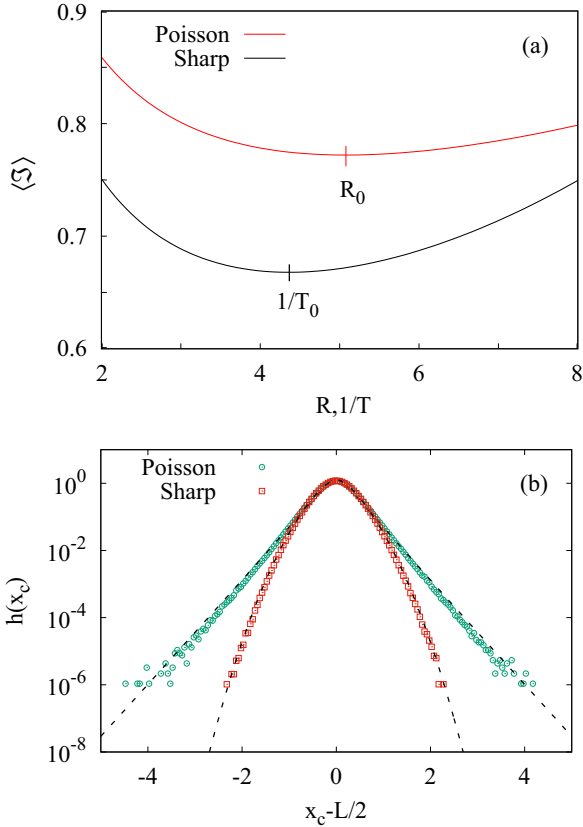
FIG. 3. (a) MFPT $\langle \mathscr{T} \rangle$ for the system of two vicious walkers under Poisson and sharp resetting. The location of the minima are marked indicating the optimal resetting rate R_0 and the optimal time of sharp reset T_0. (b) The PDF of the location of annihilation $h(x_c)$ for the two resetting protocols at their optimal values. Parameter values are $D_1, D_2 = 1$, $L = 1$, $R_0 = 5.079$, and $T_0 = 0.229$.

$T_0 \approx 0.229$ which implies $\langle \mathscr{T}_{T_0} \rangle \approx 0.668$. To get a perspective of these numbers, the diffusive timescale of the relative coordinate to cover a distance L is $\langle \mathscr{T}_D \rangle = L^2/2D_r = 0.25$ for $L = 1$. On this timescale, the MFPT for the two vicious walkers to annihilate each other is $\langle \mathscr{T}_R \rangle \approx \langle \mathscr{T}_T \rangle \approx 3\langle \mathscr{T}_D \rangle$. Furthermore, the relative advantage of sharp resetting over Poissonian resetting is $|\langle \mathscr{T}_T \rangle - \langle \mathscr{T}_R \rangle|/\langle \mathscr{T}_T \rangle \approx 0.16$, which is significant. In other words, while it is suitable for the lion to quickly hunt that both the lion and the lamb return to their homes after fixed time intervals, for the lamb Poissonian resetting is better as it might survive a little longer. We compare the two resetting protocols graphically in Fig. 3(a) and see the relative advantage of sharp resetting over Poisson resetting.

Let us now look at the tail behavior of the PDF h^t of the intersection point for Poisson and sharp resetting at their optimal levels respectively. From Eq. (12) it is clear that for Poissonian resetting $h^t_{R_0} \sim \exp\left(-\sqrt{\frac{|s_{0,R_0}| + R_0}{D_c}}|x_c - \frac{L}{2}|\right) \approx \exp(-1.78|x_c - 1/2|)$. On the other hand, for sharp resetting we have $s_{0,T_0} = \frac{1}{T_0}\ln \mathrm{erf}(\frac{L}{\sqrt{4D_r T_0}}) \approx -1.5332$. As a result, the tail part of the PDF of the location of intersection is $h^t_{T_0} \sim \exp\left(-\sqrt{\frac{|s_{0,T_0}|}{D_c}}|x_c - L/2|\right) \approx \exp(-1.75|x_c - 1/2|)$. This implies that at optimal resetting, the tails of the PDF decay faster for sharp resetting as compared to Poissonian resetting. This also follows from the fact that at optimal resetting $\langle \mathscr{T}_{T_0} \rangle < \langle \mathscr{T}_{R_0} \rangle$, as a result both the lion and the lamb do not venture far from their homes at the time of capture under sharp resetting as compared to Poissonian resetting. We compare the two PDFs both numerically and analytically in Fig. 3(b) and find that the PDF for Poissonian resetting has a higher spread as compared to that for sharp resetting.

V. CONCLUSIONS

In the realm of nonequilibrium statistical physics vicious random walkers are used to model interfacial wetting in $1 + 1$ dimensions and nonintersecting polymers. In these contexts the survival probability and the distribution of the location of coalescence are relevant quantities to address. Within the domain of capture problems, vicious random walks translate to the capture of a prey by a predator. Motivated by these examples, in this paper we study the annihilation properties of two vicious random walkers under Poissonian and sharp resetting protocols. In the absence of resetting the mean time of capture is divergent while the location of annihilation follows a Cauchy distribution. The introduction of resetting in the system renders finite MFPT due to the fact that the FPTD tails now decay exponentially as compared to algebraically in the absence of resetting. Furthermore, tails of the PDF of annihilation location now decay exponentially. This is independent of the exact nature of the resetting protocol. The central part of the PDF, however, depends on the way the system is reset to its initial location. For Poissonian resetting the central part of the PDF is a Cauchy distribution, while for sharp resetting it is a Gaussian.

We have reset the two walkers identically so that we can reduce the two-particle system as to be described by the motion of the center of mass and motion about the center of mass. We have also assumed that restarts are instantaneous, but in any realistic scenario bringing back the system to its initial state takes a finite amount of time. Even within the realm of instantaneous resetting, we chose the particles to be identical. What would happen if we include inertia and assign different masses to different particles? We explore these and other interesting possibilities in future works.

[1] W. J. Bell, *Searching Behaviour: The Behavioural Ecology of Finding Resources* (Springer Science & Business Media, Dordrecht, 2012).

[2] M. F. Shlesinger, J. Phys. A: Math. Theor. **42**, 434001 (2009).

[3] F. Bartumeus and J. Catalan, J. Phys. A: Math. Theor. **42**, 434002 (2009).

[4] O. Bénichou, C. Loverdo, M. Moreau, and R. Voituriez, Phys. Rev. E **74**, 020102(R) (2006).

[5] M. Coppey, O. Bénichou, R. Voituriez, and M. Moreau, Biophys. J. **87**, 1640 (2004).

[6] P. H. von Hippel, Annu. Rev. Biophys. Biomol. Struct. **36**, 79 (2007).

[7] J. Gorman and E. C. Greene, Nat. Struct. Mol. Biol. **15**, 768 (2008).

[8] O. Bénichou, C. Loverdo, M. Moreau, and R. Voituriez, Rev. Mod. Phys. **83**, 81 (2011).

[9] M. R. Evans, S. N. Majumdar, and G. Schehr, J. Phys. A: Math. Theor. **53**, 193001 (2020).

[10] M. Luby, A. Sinclair, and D. Zuckerman, Inf. Process. Lett. **47**, 173 (1993).

[11] H. Tong, C. Faloutsos, and J.-Y. Pan, Knowl. Inf. Syst. **14**, 327 (2008).

[12] K. Avrachenkov, A. Piunovskiy, and Y. Zhang, J. Appl. Probab. **50**, 960 (2013).

[13] L. Michaelis and M. L. Menten, Biochem. Z. **49**, 352 (1913).

[14] M. R. Evans and S. N. Majumdar, Phys. Rev. Lett. **106**, 160601 (2011).

[15] M. R. Evans and S. N. Majumdar, J. Phys. A: Math. Theor. **51**, 475003 (2018).

[16] S. Gupta, S. N. Majumdar, and G. Schehr, Phys. Rev. Lett. **112**, 220601 (2014).

[17] S. N. Majumdar, S. Sabhapandit, and G. Schehr, Phys. Rev. E **91**, 052131 (2015).

[18] R. K. Singh, K. Gorska, and T. Sandev, Phys. Rev. E **105**, 064133 (2022).

[19] S. Ahmad, I. Nayak, A. Bansal, A. Nandi, and D. Das, Phys. Rev. E **99**, 022130 (2019).

[20] S. Ahmad, K. Rijal, and D. Das, Phys. Rev. E **105**, 044134 (2022).

[21] J. Masoliver, Phys. Rev. E **99**, 012121 (2019).

[22] V. Domazetoski, A. Masó-Puigdellosas, T. Sandev, V. Méndez, A. Iomin, and L. Kocarev, Phys. Rev. Res. **2**, 033027 (2020).

[23] R. K. Singh, T. Sandev, A. Iomin, and R. Metzler, J. Phys. A: Math. Theor. **54**, 404006 (2021).

[24] M. R. Evans and S. N. Majumdar, J. Phys. A: Math. Theor. **47**, 285001 (2014).

[25] A. Nagar and S. Gupta, Phys. Rev. E **93**, 060102(R) (2016).

[26] M. R. Evans and S. N. Majumdar, J. Phys. A: Math. Theor. **44**, 435001 (2011).

[27] A. Pal, A. Kundu, and M. R. Evans, J. Phys. A: Math. Theor. **49**, 225001 (2016).

[28] A. Pal and S. Reuveni, Phys. Rev. Lett. **118**, 030603 (2017).

[29] A. Chechkin and I. M. Sokolov, Phys. Rev. Lett. **121**, 050601 (2018).

[30] I. Eliazar and S. Reuveni, J. Phys. A: Math. Theor. **53**, 405004 (2020).

[31] U. Bhat, C. De Bacco, and S. Redner, J. Stat. Mech.: Theor. Exp. (2016) 083401.

[32] T. T. da Silva and M. D. Fragoso, J. Phys. A: Math. Theor. **55**, 014003 (2022).

[33] R. Falcao and M. R. Evans, J. Stat. Mech.: Theor. Exp. (2017) 023204.

[34] E. Bertin, J. Phys. A: Math. Theor. **55**, 384007 (2022).

[35] P. L. Krapivsky and S. Redner, J. Phys. A: Math. Gen. **29**, 5347 (1996).

[36] M. R. Evans, S. N. Majumdar, and G. Schehr, J. Phys. A: Math. Theor. **55**, 274005 (2022).

[37] A. J. Bray, S. N. Majumdar, and G. Schehr, Adv. Phys. **62**, 225 (2013).

[38] M. E. Fisher, J. Stat. Phys. **34**, 667 (1984).

[39] D. A. Huse and M. E. Fisher, Phys. Rev. B **29**, 239 (1984).

[40] P. J. Forrester, J. Stat. Phys. **56**, 767 (1989).

[41] J. Baik, Commun. Pure Appl. Math. **53**, 1385 (2000).

[42] A. J. Bray and K. Winkler, J. Phys. A: Math. Gen. **37**, 5493 (2004).

[43] J. Klafter and I. M. Sokolov, *First Steps in Random Walks: From Tools to Applications* (Oxford University Press, Oxford, 2011).

[44] G. H. Weiss and R. J. Rubin, Adv. Chem. Phys. **52**, 363 (1983).

[45] J. Cardy and U. C. Täuber, Phys. Rev. Lett. **77**, 4780 (1996).

[46] M. E. Fisher and M. P. Gelfand, J. Stat. Phys. **53**, 175 (1988).

[47] G. Schehr, S. N. Majumdar, A. Comtet, and J. Randon-Furling, Phys. Rev. Lett. **101**, 150601 (2008).

[48] A. Kundu, S. N. Majumdar, and G. Schehr, J. Stat. Phys. **157**, 124 (2014).

[49] J. W. Essam and A. J. Guttmann, Phys. Rev. E **52**, 5849 (1995).

[50] J. N. Pedersen, M. S. Hansen, T. Novotný, T. Ambjörnsson, and R. Metzler, J. Chem. Phys. **130**, 164117 (2009).

[51] S. Redner and P. L. Krapivsky, Am. J. Phys. **67**, 1277 (1999).

[52] S. Reuveni, Phys. Rev. Lett. **116**, 170601 (2016).

[53] C. W. Gardiner, Springer Ser. Synergetics **13**, 3 (1985).

[54] S. Redner, *A Guide to First-Passage Processes* (Cambridge University Press, Cambridge, UK, 2001).

[55] F. Oberhettinger and L. Badii, *Tables of Laplace Transforms* (Springer Science & Business Media, Berlin, 2012).

[56] G. B. Arfken and H. J. Weber, *Mathematical Methods for Physicists*, 6th ed. (Elsevier Academic Press, New York, 2005).

[57] P. Singh and A. Pal, J. Phys. A: Math. Theor. **55**, 234001 (2022).

[58] M. Abramowitz and I. A. Stegun, *Handbook of Mathematical Functions with Formulas, Graphs, and Mathematical Tables* (Dover, New York, 1972).

[59] I. S. Gradshteyn and I. M. Ryzhik, *Table of Integrals, Series, and Products* (Academic, New York, 2014).